Two-Dimensional Analysis of a 16-μm CO_2 Downstream-Mixing Gasdynamic Laser

Purandar Chakravarty,* N. M. Reddy,† and K. P. J. Reddy‡
Indian Institute of Science, Bangalore, India

A theoretical analysis of a 16-μm CO_2-N_2-H_2 downstream-mixing gasdynamic laser, where a cold CO_2, H_2 stream is mixed with a vibrationally excited N_2 stream, tangentially downstream of the nozzle exit, is presented. The flowfield is analyzed numerically using two-dimensional, unsteady, laminar, and viscous flow modeling, including the appropriate finite-rate vibrational kinetic equations. The effect of variation of different flowfield parameters on 16-μm small-signal gain is studied and results are discussed in detail. The analysis shows that the presence of H_2 gas is detrimental to small-signal gain. The velocity ratio 1:1 between the CO_2, H_2, and N_2 mixing streams is found to be the best choice rendering local small-signal gain as high as 21.75 m^{-1} and corresponding average small-signal gain of 16.7 m^{-1} for N_2 reservoir temperature of 2000 K. These high values of small-signal gain clearly underscore the high potential which a downstream-mixing scheme has over the conventional methods for a 16-μm laser source.

Nomenclature

c_i = mass fraction of species i
c_p = specific heat at constant pressure
c_v = specific heat at constant volume
D_{12} = binary diffusion coefficient
$e^{eq}_{vib_{H_2}}$ = equilibrium vibrational energy in H_2
e_3, e_{12} = vibrational energy per unit mass of CO_2 in modes 3 and 12, respectively
e_4 = $e_{vib_{N_2}}$ = vibrational energy in mode 4 per unit mass of CO_2
e_{vib_3} = $c_{CO_2}e_3$ = vibrational energy per unit mass of the mixture in mode 3
$e_{vib_{12}}$ = $c_{CO_2}e_{12}$ = vibrational energy per unit mass of the mixture in mode 12
e_{vib_4} = $c_{N_2}e_4$ = vibrational energy in mode 4 per unit mass of the mixture.
G_0 = 16-μm small-signal gain
h = Planck's constant
k = coefficient of thermal conductivity of the mixture
Le = Lewis number computed on N_2 stream values
M = Mach number computed on N_2 stream values
N_i = population of the ith level
p = static pressure
Pr = Prandtl number, computed on N_2 stream values
Re = Reynold's number, computed on N_2 stream values
R = specific gas constant of the mixture
R_i = specific gas constant of the species i
T = static temperature
T_{vib_i} = vibrational temperature of species i
$T_{0_{N_2}}$, $P_{0_{N_2}}$ = reservoir temperature and reservoir pressure of the N_2 gas
u = x component of velocity of the mixture
$U_C : U_N$ = velocity ratio between CO_2, H_2, and N_2 streams
v = y component of velocity of the mixture
$\dot{w}_3$, $\dot{w}_4$, $\dot{w}_{12}$ = the time rate of net energy transfer into and out of modes 3, 4, and 12, respectively
X_i = mole fraction of species i
Z = molecular collision frequency
α = c_{H_2}/c_{CO_2}
γ = ratio of specific heats, computed on N_2 stream values
λ = wavelength of the laser
μ = dynamic viscosity coefficient of the mixture
ν = frequency
ρ = static density
ρ_i = density of species i
τ_{12} = radiative life time

Subscripts

(02^00), (001), (01^10) = corresponding to levels (02^00), (001), and (01^10) of CO_2
12 = combined vibrational modes 1 and 2 of CO_2
3 = vibrational mode 3 of CO_2
4 = vibrational mode 4 of N_2
R = reference (N_2 stream values are taken as reference quantities)
vib = vibrational

Received Dec. 11, 1985; revision received Sept. 16 1986.

* Research Scholar, Department of Aerospace Engineering. Student Member AIAA.
†Professor, Department of Aerospace Engineering.
‡Senior Scientific Officer, Department of Aerospace Engineering.

Introduction

THE potential use of 16-μm beam for effective laser isotope separation of Uranium[1] has evoked a lot of interest in the development of a 16-μm laser. The high efficiency, powerful performance and well developed technology of the CO_2 laser makes it an attractive candidate for the 16-μm radiation source. The 16-μm laser is obtained by using the transition between the (02^00) and (01^10) levels of CO_2 molecules. But, since the lower laser level (01^10) has a very low energy, it gets easily populated as temperature increases. Therefore cooling of the CO_2 gas is indispensable to depopulate the lower laser level (01^10), and thereby establish an efficient population inversion between the (02^00) and (01^10) levels. In this regard a CO_2-N_2-H_2 gasdynamic laser (GDL) using adiabatic expansion is the most promising candidate

because sufficient lowering of the temperature can be achieved in the laser cavity by using a large-area-ratio nozzle. Moreover, a GDL can produce high power because of its high-saturation parameter. The results of theoretical studies[2,3] for these CO_2-N_2-H_2 GDL's seem to be quite encouraging.

Although the CO_2 is the lasing gas, in conventional and premixed GDL's of the above type, the necessary pumping energy comes from vibrationally excited N_2. Thus, to have an efficient population inversion for 16-μm transition the N_2 molecules should have high vibrational energy to contribute to CO_2. In other words, to heat the N_2 gas to higher temperatures the reservoir temperature should be made high. However, there is an upper limit of approximately 2300 K for this higher temperature for premixed, conventional GDL's. Above this upper limit the CO_2 starts dissociating. Thus the small-signal gain and the specific energy of these GDL's are limited. An effective way of removing this restriction and increasing the small-signal gain and specific energy of these GDL's, is by applying the downstream-mixing scheme, where N_2 is separately heated and allowed to transfer the vibrational energy into the CO_2 in the regions of lower temperature. Since the dissociation of N_2 does not begin below 4000 K, the reservoir temperature of N_2 can safely go up to 4000 K. Thus, much more vibrational energy will be present per unit mass flow. Furthermore, the relaxation of pure N_2 in an expansion is considerably slower than that of a N_2-CO_2-H_2 mixture permitting more efficient freezing of the N_2 vibrational energy.

The preceding discussion is intended to show that the downstream-mixing GDL's have tremendous potential. However, realization of 16-μm laser using this scheme is quite complex. The lower laser level (01^10) of a CO_2 molecule considered for 16-μm generation, being low in energy, closely follows the static temperature distribution of the system. In the actual mixing region there is rise in static temperature due to total temperature recovery and consequent increase in the (01^10) level population. Thus this rise reduces the population inversion between (02^00) and (01^10) laser levels and in turn degrades the laser action. Moreover, in actual practice it takes a finite amount of time for mixing, and hence for the molecular collision to occur, before N_2 can pump the CO_2 molecules to higher levels. Furthermore, throughout the finite mixing region of the flow, vibrational deactivation will decrease the lasing action. To investigate the potential of the downstream mixing scheme for GDL's it was felt necessary to have a detailed theoretical analysis considering all these effects, in determining higher small-signal gain in the 16-μm lasing range. The present work reports this investigation.

Here the flowfield of a 16-μm downstream-mixing GDL has been analyzed using detailed two-dimensional, unsteady, viscous, laminar, and compressible flow modeling. This analysis emphasizes the fluid dynamic and kinetic aspects of the mixing flow taking into consideration the detailed collisional deactivation rate processes in the mixing region. Further, this analysis optimizes the 16-μm small-signal gain for various crucial initial parameters: e.g., different velocity ratios between the mixing streams, amount of catalyst in the gas mixture, etc. The results of the numerical study clearly show that there is a vast improvement in the downstream-mixing GDL performance over that of a conventional, premixed CO_2-N_2-H_2 GDL operating in 16-μm wavelength.

Simulation Model and Vibrational Kinetics

Figure 1 illustrates the physical set up of a downstream-mixing GDL used in the present analysis. The two nozzles shown here are a part of a bank of nozzles. Hence the two centerlines are lines of symmetry. The region of interest for the present analysis starts at the nozzle exits, extends downstream and remains confined between two centerlines. A supersonic stream of vibrationally excited N_2 is tangentially mixed with a supersonic stream of cold CO_2 and H_2 at the nozzle exits. Due to the mixing through molecular collisions,

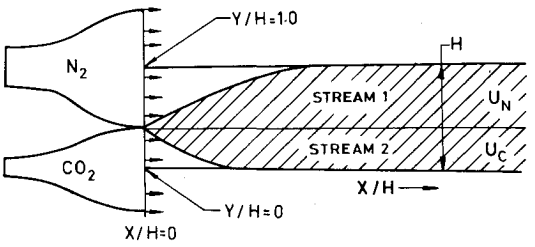

NOZZLE CONFIGURATION

		STREAM 1	STREAM 2
T	°K	141.94	141.94
T_{VIB}	°K	2000	141.94
P	N/m^2	190.5	190.5
ρ	Kg/m^3	4.522×10^{-3}	7.104×10^{-3}
MACH NO.		8.09	—

INITIAL CONDITIONS

Fig. 1 Schematic diagram of downstream-mixing gasdynamic laser and initial conditions.

vibrational energy is transferred from N_2 to cold CO_2. The N_2 vibrational temperature is assumed to be frozen during nozzle expansion, so that $T_{\text{vib}_{N_2}} = T_{0_{N_2}}$.

The nozzle sizes and pressure are chosen such that the Reynolds number is of the order of 10^3 based on the distance between the centerlines H. A laminar flow model can therefore be used. The flowfield is assumed to be two-dimensional in spatial directions X and Y as shown in Fig. 1. The steady-state values of the flowfield properties are calculated by solving the unsteady, two-dimensional, Navier-Stokes equations augmented with appropriate vibrational relaxation equations, using an explicit, time-dependent, second-order accurate, finite-difference, computer code.[4] This code is patterned after the predictor–corrector approach of MacCormack. These steady-state values of the flowfield properties are further used for calculating the population inversion and small-signal gain for the 16-μm CO_2-N_2-H_2 downstream-mixing GDL.

Figure 2 shows that CO_2, being a linear triatomic molecule, has three fundamental modes of vibration, having frequency ν_1, ν_2, ν_3 with vibrational energies e_1, e_2, e_3 and corresponding local equilibrium temperatures T_1, T_2, and T_3. N_2, being a diatomic molecule, has only one mode of vibration with fundamental frequency of ν_4 and the corresponding energy and temperature e_4 and T_4, respectively.

When the vibrationally excited N_2 is allowed to mix with cold CO_2 in a CO_2-N_2-H_2 downstream-mixing GDL, vibrational energy is transfered from N_2 to CO_2, due to molecular collision. This energy transfer takes place in three ways[5] viz., translational-vibrational (T-V) transfer of both inter and intramolecular type, vibrational-vibrational (V-V) transfer of intermolecular type, and vibrational-vibrational (V-V) transfer of intramolecular type. Since a 16-μm transition is obtained between (02^00) and (01^10) levels of CO_2, the study of 16-μm kinetics of CO_2 involves, the question of populating (001) and depopulating (01^10) levels and then populating (02^00) level by depopulating (001) level. The population of the (001) level and (010) level depends on the kind of energy transfer processes described above. The processes involved can be expressed as:

T-V processes:

$$CO_2(010) + M \rightleftharpoons CO_2(000) + M + 667\ \text{cm}^{-1} \quad (1)$$

$$N_2(V=1) + M \rightleftharpoons N_2(V=0) + M + 2331\ \text{cm}^{-1} \quad (2)$$

V-V processes, intermolecular:

$$CO_2(001) + N_2 \rightleftharpoons CO_2(000) + N_2(V=1) + 18\ cm^{-1} \quad (3)$$

V-V processes, intramolecular:

$$CO_2(001) + M \rightleftharpoons CO_2(030) + M + 416\ cm^{-1} \quad (4)$$

$$CO_2(100) + M \rightleftharpoons CO_2(020) + M + 102\ cm^{-1} \quad (5)$$

M stands for collision partner which can be CO_2, N_2, or H_2. The following observations can be made from these reactions:

1) The (001) level of CO_2 and ($V=1$) level of N_2 have almost the same energy, differing by only 18 cm^{-1}. Reaction (3) takes place very fast because of this very near resonance energy transfer between these two modes. This reaction is called the "pumping reaction."

2) The population of the (001) level of CO_2 depends on the population of the ($V=1$) level of N_2 through reaction (3). In addition, it also depends on reaction (4) and 9.4-μm laser stimulation, which together tend to deplete the (001) level.

3) The levels (100) and (020) of CO_2 are relatively close in energy. The existence of Fermi resonance between these makes the reaction (5) very fast.

4) The population of (010) level is dependent on the rate of 16-μm laser power extraction, which tends to fill the level. Further, it also depends on reaction (1) which depopulates it.

Effective populations of (020) level and the (010) level are further tailored in the present lasing system for the generation of a 16-μm beam. It is done initially, by cooling the CO_2 to depopulate the (010) level via reaction (1) and then, by injecting an intense, saturating laser pulse of 9.4-μm into the CO_2-N_2 mixture. This injection populates the (02^00) level by depopulating (001) level, thereby creating a population inversion between (02^00) and (01^10) levels. However, the actual population of (02^00) level depend not only on the intensity and temporal width of the stimulating 9.4-μm radiation but also on the rate of de-excitation through the following reactions:

$$CO_2(02^00) + M \rightleftharpoons CO_2(10^00) + M - 102.8\ cm^{-1} \quad (6)$$

$$CO_2(02^00) + M \rightleftharpoons CO_2(02^20) + M - 49.9\ cm^{-1} \quad (7)$$

$$CO_2(02^00) + CO_2(00^00) \rightleftharpoons 2CO_2(01^10) - 50.1\ cm^{-1} \quad (8)$$

The reaction times for these reactions are approximately 1.3 μs, 480 ns, and 4.2 μs, respectively. Therefore, to populate the (02^00) level while avoiding de-excitation through these reactions, a sufficiently intense and saturating 9.4-μm laser pulse having pulse duration shorter than the time of the above reactions is injected into the system. This process can be expressed as:

$$CO_2(001) + h\nu \quad (\lambda = 9.4\ \mu m) \rightarrow CO_2(02^00) + 2h\nu \quad (9)$$

Since the pulse duration of such a 9.4-μm laser is much shorter than the relaxation time of the (001) level, the contribution to the population of the (02^00) level from (001) level through spontaneous emission can be safely neglected. Hence, under these conditions the population of (02^00) level, as pointed out by Suzuki et al.,[2] will be:

$$N_{02^00} = 0.5(N'_{02^00} + N_{001}) \quad (10)$$

Here N'_{02^00} and N_{001} are the initial population of (02^00) and (001) levels of CO_2.

The above discussion makes it clear that the most important rate-determining step for the generation of 16-μm laser is the amount of vibrational-energy transfer from N_2 ($V=1$) level to CO_2 (001) level. In a downstream-mixing GDL it takes a finite amount of time for the molecular collision to occur and for the energy transfer to take place. Therefore, in the present analysis, we have used the detailed vibrational kinetic model of Munjee,[6] where ν_3 mode of CO_2 and ν_4 mode of N_2 are separately dealt with. In this model ν_1 and ν_2 modes of CO_2 are combined together to become ν_{12} on the basis of local equilibrium between them, achieved through Fermi resonance [Eq. (5)]. Hence the effective vibrational energy e_{12} is equal to $e_1 + 2e_2$ and $T_{12} = T_1 = T_2$. Thus there are three modes, namely: mode 12, mode 3, and mode 4, as shown in Fig. 2. The expressions for the time rate of net energy transfer into and out of these modes, $\dot{w}_{12}$, $\dot{w}_3$, and $\dot{w}_4$, can be obtained from Ref. 6 or Ref. 7.

Governing Equations

In the present analysis two streams are considered to be compressible and viscous, with variations in viscosity, thermal conductivity and diffusivity. They are also nonradiating and have nonequilibrium vibrational energy exchange between themselves. The study takes only laminar mixing into consideration. The basic set of equations used comprise unsteady, two-dimensional, laminar, Navier-Stokes equations augmented with appropriate vibrational relaxation equations. These governing equations are derived on the basis of following assumptions:

1) The effect of pressure and temperature gradients on diffusion flux velocities is small enough to be neglected. Only the effect of concentration gradients on the diffusion fluxes as related by Fick's law is important enough for consideration.

2) The concentration of H_2 is negligibly small compared to CO_2 and N_2 concentration in the mixture and hence the mixture can be treated as a binary mixture of CO_2 and N_2 with a single binary diffusion coefficient.

3) The H_2 vibrational modes are in equilibrium with the translational modes of the gas mixture.

The equations derived are further nondimensionalized using the N_2 stream values at the nozzle exit as reference quantities. The spatial directions are nondimensionalized using the parameter H (the distance between the centerlines of the two nozzles). The characteristic reference time is defined as $t_R = H/u_R$, where u_R is the reference velocity, i.e., velocity of the N_2 stream. The final equations in the nondimensional form are:

Continuity:

$$\frac{\partial \rho}{\partial t} = -\left[\frac{\partial}{\partial x}(\rho u) + \frac{\partial}{\partial y}(\rho v)\right] \quad (11)$$

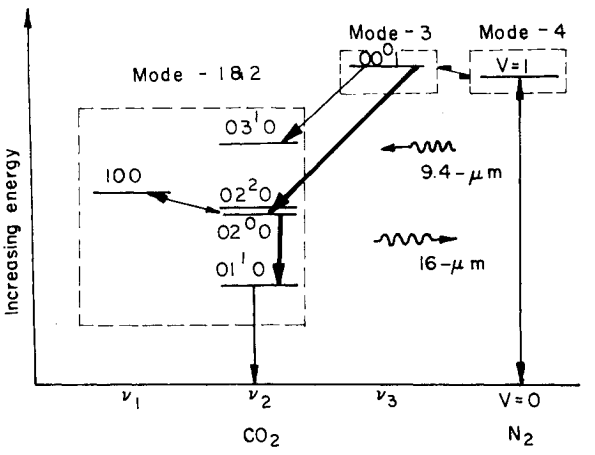

Fig. 2 Schematic diagram showing the grouping of energy levels in three modes for Munjee's Model and also the transition for 16-μm laser emission.

Species continuity:

$$\frac{\partial}{\partial t}(\rho c_{N_2}) = -\frac{\partial}{\partial x}\left[\rho u c_{N_2} - \left(\frac{Le}{PrRe}\right)\rho D_{12}\frac{\partial c_{N_2}}{\partial x}\right] - \frac{\partial}{\partial y}\left[\rho v c_{N_2} - \left(\frac{Le}{PrRe}\right)\rho D_{12}\frac{\partial c_{N_2}}{\partial y}\right] \quad (12)$$

x momentum:

$$\frac{\partial}{\partial t}(\rho u) = -\frac{\partial}{\partial x}\left[\rho uu + \frac{p}{\gamma M^2} + \frac{2}{3}\frac{\mu}{Re}\left(\frac{\partial u}{\partial x} + \frac{\partial v}{\partial y}\right) - \frac{2\mu}{Re}\frac{\partial u}{\partial x}\right] - \frac{\partial}{\partial y}\left[\rho uw - \frac{\mu}{Re}\left(\frac{\partial u}{\partial y} + \frac{\partial v}{\partial x}\right)\right] \quad (13)$$

y momentum:

$$\frac{\partial}{\partial t}(\rho v) = -\frac{\partial}{\partial x}\left[\rho vu - \frac{\mu}{Re}\left(\frac{\partial u}{\partial y} + \frac{\partial v}{\partial x}\right)\right] - \frac{\partial}{\partial y}\left[\rho vv + \frac{p}{\gamma M^2} - \frac{2\mu}{Re}\frac{\partial v}{\partial y} + \frac{2}{3}\frac{\mu}{Re}\left(\frac{\partial u}{\partial x} + \frac{\partial v}{\partial y}\right)\right] \quad (14)$$

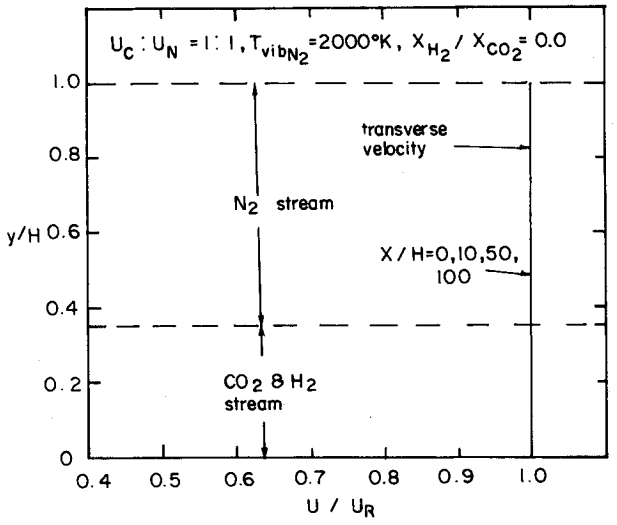

Fig. 3 Transverse velocity distribution profiles at various axial locations in the cavity.

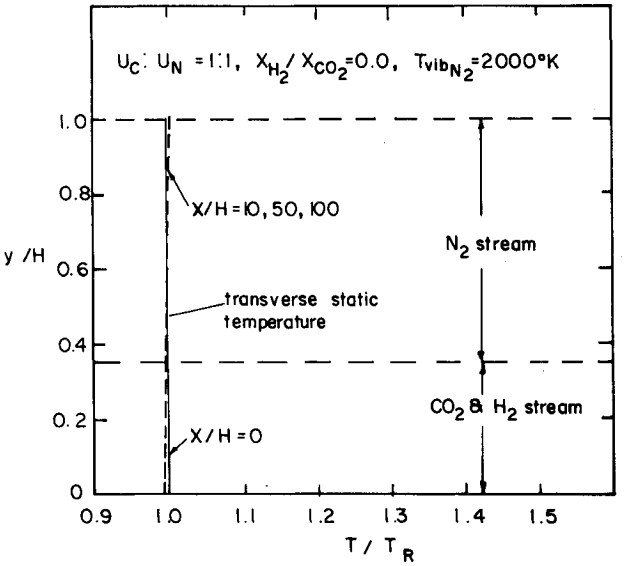

Fig. 4 Transverse static temperature distribution profiles at various axial locations in the cavity.

Energy:

$$\frac{1}{\gamma}\rho c_v\frac{\partial T}{\partial t} - \left(\frac{\gamma-1}{\gamma}\right)\left[RT\frac{\partial \rho}{\partial t} + \rho T\frac{\partial c_{N_2}}{\partial t}(R_{N_2} - R_2)\right] = -\left[\rho u c_p\frac{\partial T}{\partial x} + \rho v c_p\frac{\partial T}{\partial y}\right] - \left(\frac{\gamma-1}{\gamma}\right)\left[\rho_{CO_2}(\dot{w}_{12} + \dot{w}_3) + \rho_{N_2}\dot{w}_4\right] + \frac{1}{(PrRe)}\left[\frac{\partial}{\partial x}\left(k\frac{\partial T}{\partial x}\right) + \frac{\partial}{\partial y}\left(k\frac{\partial T}{\partial y}\right)\right] + \left(\frac{\gamma-1}{\gamma}\right)\left[u\frac{\partial p}{\partial x} + v\frac{\partial p}{\partial y}\right] + \frac{(\gamma-1)M^2}{Re}\mu\left[2\left\{\left(\frac{\partial u}{\partial x}\right)^2 + \left(\frac{\partial v}{\partial y}\right)^2\right\} + \left(\frac{\partial v}{\partial x} + \frac{\partial u}{\partial y}\right)^2 - \frac{2}{3}\left(\frac{\partial u}{\partial x} + \frac{\partial v}{\partial y}\right)^2\right] + \frac{Le}{PrRe}\left(\frac{\gamma-1}{\gamma}\right) \times \rho D_{12}\left[\frac{7}{2}\left(R_{N_2} - \frac{R_{CO_2}}{1+\alpha}\right) - \frac{\alpha}{1+\alpha}\left(\frac{7}{2}R_{H_2} + \frac{\partial e_{vib_{H_2}}}{\partial T}\right)\right] \times \left[\frac{\partial c_{N_2}}{\partial x}\frac{\partial T}{\partial x} + \frac{\partial c_{N_2}}{\partial y}\frac{\partial T}{\partial y}\right] \quad (15)$$

Equation of state:

$$p = \rho RT \quad (16)$$

Vibrational Relaxation Equations

These equations refer to a flowing system, where vibrational energy in a given mode changes not only due to collisions but also due to convection and viscous diffusion. These are represented as:

$$\frac{\partial}{\partial t}(\rho e_{vib_{12}}) = -\frac{\partial}{\partial x}\left[\rho u e_{vib_{12}} + \left(\frac{Le}{PrRe}\right)\rho D_{12}\frac{\partial c_{N_2}}{\partial x}\frac{e_{12}}{1+\alpha}\right] - \frac{\partial}{\partial y}\left[\rho v e_{vib_{12}} + \left(\frac{Le}{PrRe}\right)\rho D_{12}\frac{\partial c_{N_2}}{\partial y}\frac{e_{12}}{1+\alpha}\right] + \rho_{CO_2}\dot{w}_{12} \quad (17)$$

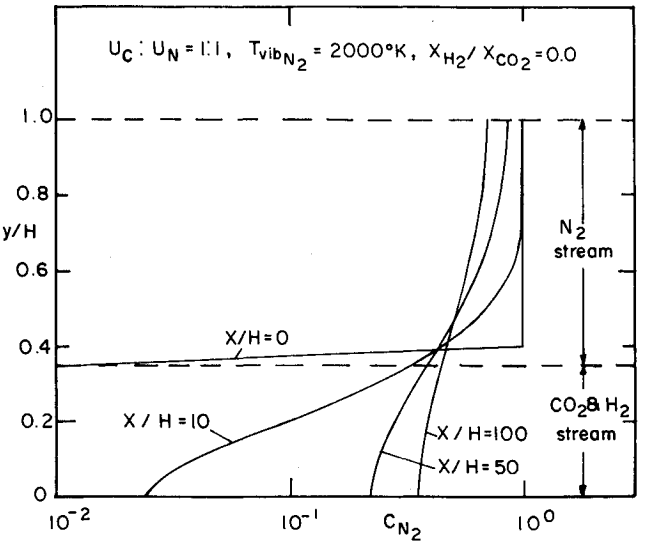

Fig. 5 Transverse nitrogen mass-fraction profiles at various axial locations in the cavity.

$$\frac{\partial}{\partial t}(\rho e_{\text{vib}_3}) = -\frac{\partial}{\partial x}\left[\rho u e_{\text{vib}_3} + \left(\frac{Le}{PrRe}\right)\rho D_{12}\frac{\partial c_{N_2}}{\partial x}\frac{e_3}{1+\alpha}\right] - \frac{\partial}{\partial y}\left[\rho v e_{\text{vib}_3} + \left(\frac{Le}{PrRe}\right)\rho D_{12}\frac{\partial c_{N_2}}{\partial y}\frac{e_3}{1+\alpha}\right] + \rho_{CO_2}\dot{w}_3 \tag{18}$$

$$\frac{\partial}{\partial t}(\rho e_{\text{vib}_4}) = -\frac{\partial}{\partial x}\left[\rho u e_{\text{vib}_4} - \left(\frac{Le}{PrRe}\right)\rho D_{12}\frac{\partial c_{N_2}}{\partial x}e_4\right] - \frac{\partial}{\partial y}\left[\rho v e_{\text{vib}_4} - \left(\frac{Le}{PrRe}\right)\rho D_{12}\frac{\partial c_{N_2}}{\partial y}e_4\right] + \rho_{N_2}\dot{w}_4 \tag{19}$$

Mixture properties are calculated following Parthasarathy et al.[4] A few additional terms used in the above equations are:

$$R = c_{N_2}R_{N_2} + c_{CO_2}R_{CO_2} + c_{H_2}R_{H_2}$$

$$R_2 = \frac{R_{CO_2}}{1+\alpha} + \frac{\alpha}{1+\alpha}R_{H_2}$$

$$c_v = \frac{5}{2}R_{N_2}c_{N_2} + \frac{5}{2}R_{CO_2}c_{CO_2} + c_{H_2}\left(\frac{5}{2}R_{H_2} + \frac{\partial e^{eq}_{\text{vib}_{H_2}}}{\partial T}\right)$$

Population Inversion and Small-Signal Gain

Equation (10) is used along with the steady-state values of the flowfield variables for calculating the population inversion between (02^00) and (01^10) levels as well as the 16-μm small-signal gain. The expression for small-signal gain for 16-μm transition, i.e., $P(15)$ line of (02^00)–(01^10) transition, after the rotational correction is:

$$G_0 = \frac{\lambda^2}{4\pi\tau_{12}Z}\left(\frac{34.7906}{T}\right)(N_{02^00} - N_{01^10}) \times \exp(-134.67313/T) \tag{20}$$

Results and Discussion

The numerical technique used in the present analysis is an explicit, time-dependent, second-order accurate, finite-difference technique. The results reported here are the final steady-state values which are of relevance to issues investigated within the scope of the present study. Here the 16-μm small-signal gain is calculated at different stations downstream of the nozzle exits, on the assumption that a highly intense and saturating 9.4-μm laser pulse is injected uniformly at these stations. The initial conditions used are given in Fig. 1.

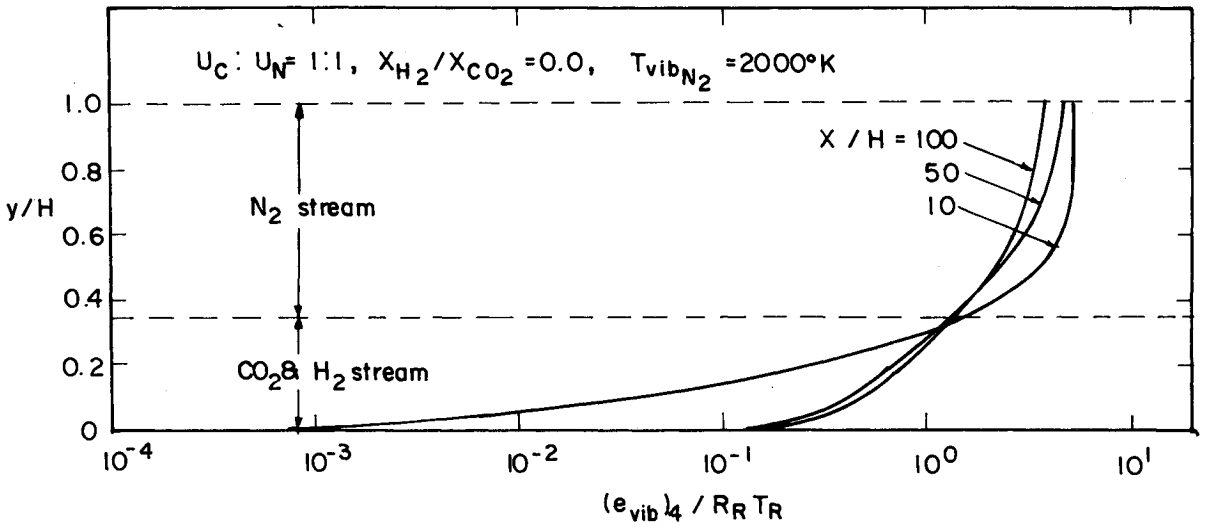

Fig. 6 Transverse profiles of vibrational energy in mode 4 at various axial locations in the cavity.

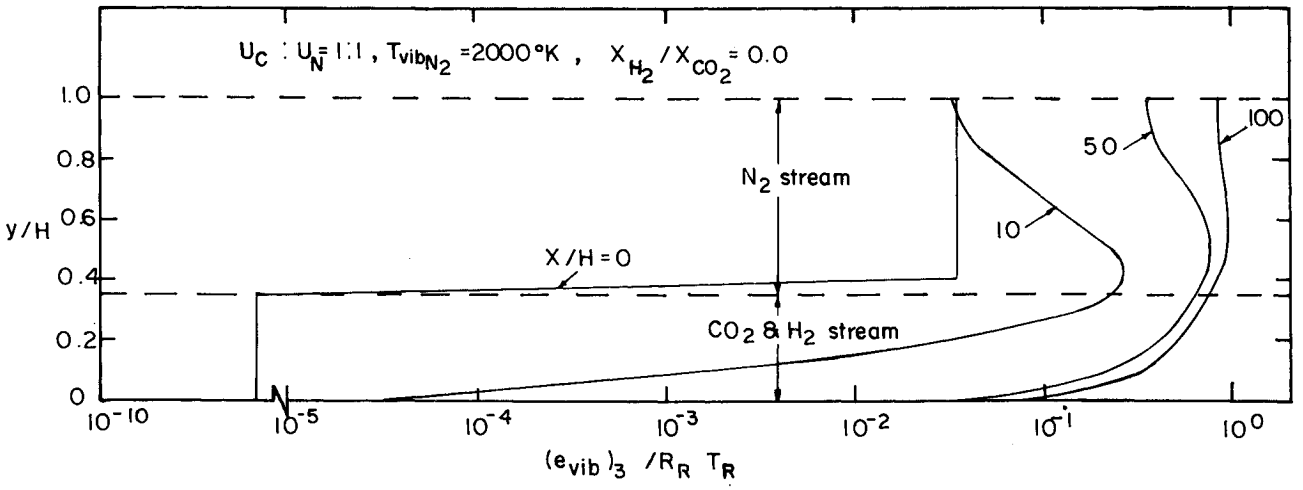

Fig. 7 Transverse profiles of vibrational energy in mode 3 at various axial locations in the cavity.

Optimization of 16-μm small-signal gain has also been attempted in the present analysis. This has been done with respect to various crucial parameters. The study involved an investigation of:

1) The effect of velocity ratios between the two mixing streams on the small-signal gain (essentially three velocity ratios have been chosen: 1:1, 1:2, 2:1).

2) The effect of H_2 as a catalyst on the small-signal gain.

During computation, grid points in the transverse direction have been assumed such that the $CO_2 + H_2$ stream extends from $Y/H = 0$ to $Y/H = 0.35$, and there is only the N_2 stream beyond this range.

Steady-state, transverse velocity distribution profiles of the system of Fig. 1 having velocity ratio $U_C : U_N = 1:1$ are shown in Fig. 3. Here it can be observed that there is no velocity discontinuity, even far downstream at $X/H = 100$. Further, Fig. 4 represents the transverse static temperature distribution profiles across the cavity at various X/H locations. Here again we observe that in the case of $U_C : U_N = 1:1$, there is no meaningful increase in the static temperature even at $X/H = 100$. This is due to the fact that the effect of viscous dissipation in increasing the static temperature has been eliminated because there is no velocity discontinuity between the two streams. The mixing of two streams in this case is only by diffusion. Hence there is no appreciable rise in the static temperature.

The nitrogen mass-fraction profiles are represented in Fig. 5. The strong gradients of N_2 concentrations near the inlet act as a driving potential to cause a rapid diffusion of nitrogen into the lower stream of CO_2 and H_2. Due to this, an almost uniform profile evolves at $X/H = 100$. This uniformity of the flowfield is advantageous in ensuring the optical quality of the laser beam.

The vibrational energy profiles are represented in Figs. 6, 7, and 8. The vibrational energy transfer, as pointed out in the section on kinetics, is a complex phenomenon. Furthermore, the vibrational energy of a molecule inside a moving fluid element in the mixing flowfield is changed by convection and diffusion across the fluid element boundaries and by vibrational energy exchange with other molecules that are inside the fluid element as well as with those that diffuse across the boundaries.

Figure 6 represents the profiles of vibrational energy in mode 4. The effect of N_2 diffusion in the lower CO_2 and H_2 stream can be clearly seen, as the e_{vib_4} increase from a very low value at $Y/H = 0$ and $X/H = 10$ to an appreciably higher one at $Y/H = 0$ and $X/H = 100$. On the other hand, due to the existence of N_2 in the upper stream, e_{vib_4} does not change appreciably, a fact that is reflected in the upper portion of the curve.

Profiles of vibrational energy in mode 3 are represented in Fig. 7. These profiles of e_{vib_3} are the direct measure of the population in the (001) level of CO_2, which, on injection of 9.4-μm laser pulse, populates the (02^00) level. Thus, higher e_{vib_3} means higher gain for 16-μm lasing. Here at $X/H = 0$, up to $Y/H = 0.35$ the e_{vib_3} is very small, which implies that in a downstream-mixing GDL at the exit of the nozzle, CO_2 is very cold and hence mode 3 is practically empty. However, at $Y/H = 0.4$ onward (at the same $X/H = 0$) there is a large increase in e_{vib_3}. This is due to the fact that, in the process of attainment of steady state at $X/H = 0$, during the time elapsed, a few of the CO_2 molecules diffuse into the N_2 stream. There is a large increase in e_{vib_3} at far downstream due to mixing at $X/H = 100$ and $Y/H = 0$. From $Y/H = 0.4$ and upward, distribution of e_{vib_3} is uniform.

Figure 8 is a representation of the profiles of vibrational energy in mode 12. The plots here are very important because 16-μm lasing involves lower vibrational modes of CO_2, i.e., mode 12. This mode, due to its lower energy level, is in near equilibrium with the translational mode. The curves reflect the changes in the static temperature T, which as in Fig. 4, is

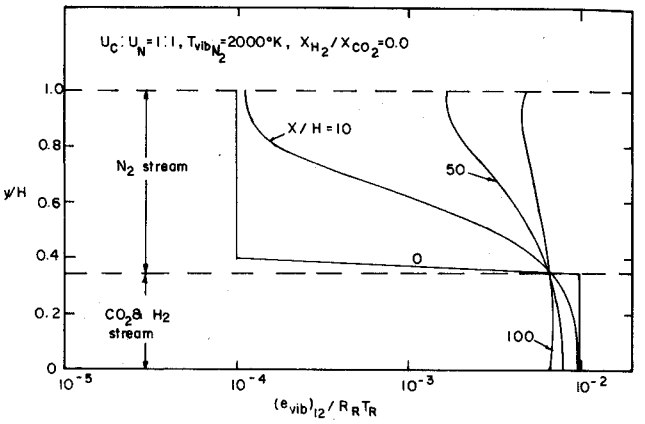

Fig. 8 Transverse profiles of vibrational energy in mode 12 at various axial locations in the cavity.

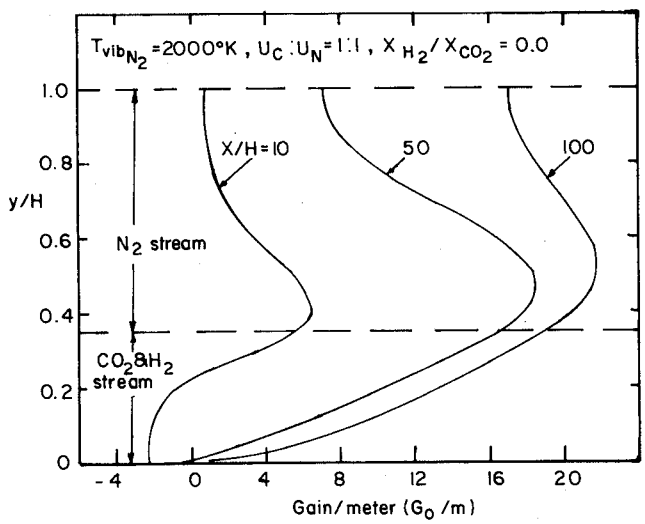

Fig. 9 Transverse profiles of local small-signal gain at various axial locations in the cavity.

indicated as negligible below the centerline. In the N_2 region, i.e., above the centerline at $X/H = 0$ to 10, there are very few CO_2 molecules and hence $e_{vib_{12}}$ is low. The $e_{vib_{12}}$ above centerline increases at $X/H = 100$ due to mixing.

A measure of the population inversion is reflected in the local small-signal gain profiles of Fig. 9. The small-signal gain (G_0) usually starts from a negative value (a state of no population inversion), approaches a positive value (a state of population inversion) and reaches a peak before coming down. Considering this with respect to the geometry of Fig. 1, the illustration phenomenon can be explained in the following way. Moving along the direction transverse to the flow shows that at $Y/H = 0$ there are very few excited CO_2 molecules in the (02^00) level, so G_0 is negative. Between $Y/H = 0.35$ to $Y/H = 0.7$, there is good mixing and hence a larger number of excited CO_2 molecules are available, so G_0 increases. By similar reasoning, G_0 decreases in the region $Y/H = 0.7$ to $Y/H = 1.0$ due to nonavailability of a larger number of excited CO_2 molecules. Another important feature is that the strong gradients of G_0 are attenuated as the stream mixes further downstream. At $X/H = 100$ the gain is more uniform, as is shown by the upper portion of the curve. This reflects the point that far downstream, the flow gradually tends towards that of a conventional 16-μm GDL. An important difference between the conventional 16-μm GDL's and the present one is the local small-signal gain G_0. It is 21.75 m^{-1} at $X/H = 100$ in the present case, which is about 6.80 times higher than the highest value reported to date, i.e., 3.2 m^{-1} by Horioka et al.[3]

in the case of the former. The present value is also 1.45 times higher than the best reported value of 14.9 m^{-1} by Velikanov et al.[8] for downstream-mixing 16-μm GDL with a N_2 reservoir temperature of 2500 K. This high value of G_0 at N_2 reservoir temperature of 2000 K in the present case is obtained even when the detailed collisional deactivation rate processes in the mixing zone are taken into consideration. In addition these values of small-signal gain are higher than values obtained in Ref. 9 from theoretical analysis of a 16-μm downstream-mixing GDL. This may be because their analysis is quasi-one-dimensional and inviscid, with no consideration for mixture diffusivity, thermal conductivity and relative velocity between N_2 and CO_2 mixing streams.

Integrating the profiles given in Fig. 9 individually along Y/H, a profile of gain can be obtained for a particular X location. This is a representation of average small-signal gain, and can be used to express the overall laser quality of the mixing flow. Such a profile is given in the topmost plot in Fig. 10. Here it can be observed that while in Fig. 9 at $X/H = 100$ G_0 was 21.75 m^{-1}, in Fig. 10 at $X/H = 100$ the G_0 is 16.7 m^{-1}. This is still higher than the best reported value of the downstream mixing GDL by Velikanov et al.[8]

The integrated gain gradually tends to become constant downstream of $X/H = 60$, which contributes to good laser quality. These curves also clearly demonstrate that velocity ratio $U_C : U_N = 1:1$ between the two streams gives rise to maximum gain, a feature which supports the earlier contention. This occurs because static temperature increases caused by viscous dissipation are eliminated, and the mixing is totally by diffusion. Further, diffusion of vibrational species across the fluid element boundaries are also minimized due to lack of significant velocity gradients.

In conventional CO_2 GDL, it is found that addition of H_2 gas into the laser gas mixture leads to an increase of small-signal gain. Hence an investigation was undertaken to study the effect of H_2 on the performance of downstream-mixed CO_2 GDL. The results are plotted in Fig. 11. The curves clearly indicate that in contrast to the conventional GDL, addition of H_2 gas is deleterious to the performance of downstream-mixing GDL. Physically, this effect is due to the following reasons. In a conventional GDL, there is some population of the lower laser level. If left alone, this would tend to decrease laser gain. The addition of H_2 effectively depopulates the lower level thereby increasing laser gain. In the case of downstream-mixing GDL, as the CO_2 is selectively excited to the higher laser level, the lower laser level is virtually empty and hence H_2 added to the laser gas mixture acts only as a contaminant which results in the reduction of CO_2 energy because of molecular collisions. This leads to the decrease in small-signal gain as shown in Fig. 11. Similar experimental results were also obtained by Hoffmann et al.[10] but for 10.6-μm downstream-mixing GDL using different mixtures of H_2, CO_2 and N_2.

In the context of power extraction, H_2 does have some beneficial effect on the 16-μm downstream-mixing GDL's. Under experimental conditions, when the laser power is extracted from the cavity, the CO_2 molecules that are in (02^00) level give out radiation and decay down to (01^10) level. An H_2 additive depopulates the lower level, helping to maintain a population inversion for a longer period of time. Although H_2 is detrimental to small-signal gain, it is beneficial for power extraction. This conclusion was obtained from experience with a downstream-mixing GDL operating in 10.6-μm range.[4]

The effect of N_2 reservoir temperature variations on 16-μm small-signal gain has also been studied in detail. It has been observed that for 16-μm laser operation, the integrated small-signal gain decreases with the increase in the vibrational temperature of N_2 gas. A detailed discussion of the effects of N_2 reservoir temperature on the small-signal gain of 16-μm CO_2 downstream-mixing GDL is presented in Ref. 11.

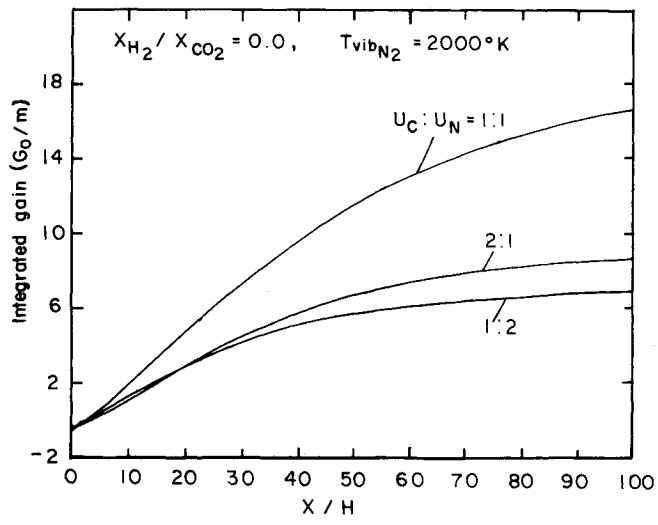

Fig. 10 Variation of average small-signal gain (integrated gain) with distance along the flow for different velocity ratios.

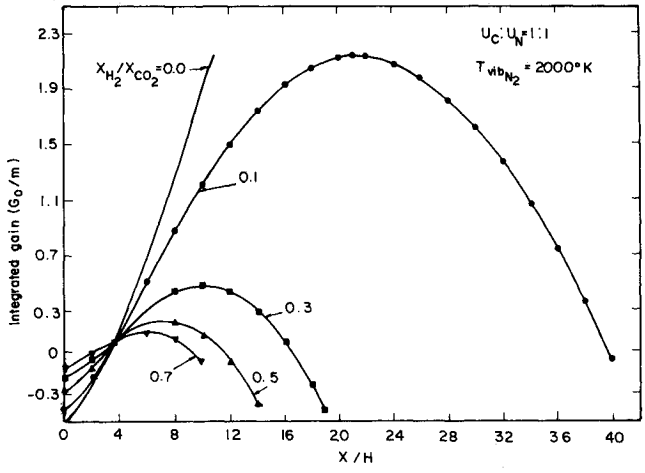

Fig. 11 Variation of average small-signal gain (integrated gain) with distance along the flow for different H_2 contents.

Conclusions

From the preceding discussions the following conclusions can be made.

1) The large values of local small-signal gain and integrated small-signal gain obtained from this analysis clearly illustrate the high potential of CO_2–N_2–H_2 downstream-mixing GDL as the best laser source in the 16-μm range for industrial applications at present.

2) A 1:1 velocity ratio between the two mixing streams appears to be ideal for minimizing viscous heating and obtaining high small-signal gain.

3) Though maximum small-signal gain is achieved in the absence of H_2 as catalyst, its presence is necessary to ensure efficient power extraction.

4) Although laminar mixing is slow, it is very efficient because it creates uniformly mixed regions with homogeneous density distributions even at large distance from the inlet to the laser cavity.

References

[1]Eerkens, J.W., "Spectral Considerations in the Laser Isotope Separation of Uranium Hexafluride," *Applied Physics*, Vol. 10, 1976, pp. 15–31.

[2]Suzuki, K., Saito, S., Obara, M., and Fujioka, T., "Theoretical Study for a 16-μm CO_2 Gasdynamic Laser," *Journal of Applied Physics*, Vol. 51, Aug. 1980, pp. 4003–4009.

[3]Horioka, K., Kanazawa, H., and Kasuya, K., "Effect of Nozzle Geometry on the Performance of 16-μm CO_2 Gasdynamic Lasers," (in Japanese) *Review of Laser Engineering*, Vol. 10, 1982, pp. 479–486.

[4]Parthasarathy, K.N., Anderson, J.D., Jr., and Jones, E., "Downstream-Mixing Gasdynamic Lasers—A Numerical Solution," *AIAA Journal*, Vol. 17, Nov. 1979, pp. 1208–1215.

[5]Taylor, R.L. and Bitterman, S., "Survey of Vibrational Relaxation Data for Processes Important in the CO_2–N_2 Laser System," *Review of Modern Physics*, Vol. 41, Jan. 1969, pp. 26–47.

[6]Munjee, S.A., "Numerical Analysis of a Gasdynamic Laser Mixture," *The Physics of Fluids*, Vol. 15, March 1972, pp. 506–508.

[7]Anderson, J.D., Jr., *Gasdynamic Lasers: An Introduction*, Academic Press, New York, 1976, pp. 21–33.

[8]Velikanov, A.G., Gorshunov, N.M., Neshchimenko, Yu. P., and Shcherbo, A.B., "Comprehensive Optimization of Gasdynamic Laser Parameters for Maximum Gain in the 16-μ Band," *Soviet Journal of Quantum Electronics*, Vol. 10, Oct. 1980, pp. 1292–1294.

[9]Masuda, W. and Yamada, H., "Theoretical Analysis of a 16-μm CO_2 Downstream-Mixing Gasdynamic Laser," 5th International Symposium on Gas Flow and Chemical Lasers, Oxford, England, Aug. 1984.

[10]Hoffmann, P., Hügel, H., and Schall, W., "Contaminants in a Gasdynamic Mixing Laser," *AIAA Journal*, Vol. 15, Oct. 1977, pp. 1527–1529.

[11]Chakravarty, P., Reddy, N.M., and Reddy, K.P.J., "A Study of the Effect of N_2 Reservoir Temperature on a 16-μm CO_2–N_2 Downstream-Mixing Gasdynamic Laser," *Optics Communications*, Vol. 58, May 1986, pp. 130–132.